Effect of Experimental Conditions on the Non-Repeatability of Temperature Measurements During the "Spark Plasma Sintering Process"

Youssef ACHENANI[1], Abdelkhalek CHEDDADI[1,*], Malika SAÂDAOUI[1], Guillaume BONNEFONT[2], Gilbert FANTOZZI[2]

[1] Mohammed V University in Rabat, Mohammadia School of Engineers, Avenue Ibn Sina, P.O. Box 765-Agdal, Rabat, Morocco

[2] Lyon University, National Institute of Applied Sciences of Lyon, MATEIS Laboratory, UMR 5510 CNRS, 20 Avenue Albert Einstein, F-69621 Villeurbanne Cedex, France

[*] **Corresponding author:** E-mail: cheddadi@emi.ac.ma

Abstract

In this study, we investigate the experimental conditions influencing the reproducibility of temperature measurements such as the temperature control location and the die asymmetric location relatively to the sample. In this context, we used a finite element modeling (FEM) and a series of experiments under temperature control mode to check the repeatability of the temperature measurements during SPS sintering and also allows to evaluate the robustness of the present model. An alumina sample was studied as an electrically insulator ceramic material. A thermal sintering cycle is imposed using a control pyrometer of temperature on the top graphite punch near the sample.

Keywords: *Spark Plasma Sintering; Finite element modeling; Temperature measurements; Reproducibility*

1-Introduction

The Spark Plasma Sintering (SPS) process is one of the most attractive techniques for powders consolidation under the effects of pulsed electrical current and uniaxial pressure to the graphite die containing the sintered samples. The efficiency of SPS in comparison to other conventional hot pressing methods (HP, HIP), that the sintering is achieved more quickly by the inner heating generated in the whole set-up by Joule effect. Therefore, it preserves the ultrafine microstructure, that characterizes the nanopowders as-received, permitting to ensure the improved mechanical, physical or optical properties. This process has become a powerful technology to manufacture high quality ceramics including nanostructured ceramics [1,2]. The temperature measurement is a quantitative experimental information for the materials densification by SPS process and considered a decisive parameter on obtained final properties for the sintered samples. In many studies carried out on the predictive modeling of temperature distribution in the SPS technology, the discrepancy noted between modeled and measured temperature at measuring points in different research results could be due to uncertainties over the true temperature measurements under the retained experimental conditions [3] and the reliability of numerical models associated to simplifying assumptions [4]. In this work, a finite element modeling was used to simulate the experimental conditions influencing the non-reproducibility of temperature measurements during SPS process. A series of experiments were run to validate the numerical model. Special attention was drawn to the location of the light beam alignment outputted from the axial optical pyrometer at desired point for temperature control and also the shift upward or downward of the die relatively to the sample. The following physical quantities have been systematically controlled: (i)-The maximum temperature reached at the sample center, (ii)-The radial temperature distributions and (iii)-The radial thermal gradients present within specimens.

2-Numerical modeling

Finite element modeling was performed using the software COMSOL Multiphysics® to simulate the thermoelectric coupling during SPS sintering. The Joule heating model obeys to the heat (Eq. 1) and the electric current (Eq. 2) equations given in the cylindrical coordinates (r, z):

$$\rho c_p \frac{\partial T}{\partial t} = \frac{1}{r}\frac{\partial}{\partial r}\left(r k_r \frac{\partial T}{\partial r}\right) + \frac{1}{z}\frac{\partial}{\partial z}\left(r k_z \frac{\partial T}{\partial z}\right) + \dot{q}_i \quad (1)$$

$$\frac{1}{r}\frac{\partial (r i_r)}{\partial r} + \frac{\partial i_z}{\partial z} = 0 \quad (2)$$

where ρ, c_p, k_r and k_z, represent respectively the density, the specific heat, the thermal conductivity in r and z directions. $\dot{q}_i$ is the heat generated by Joule heating per unit volume per unit time, i_r and i_z represent the current density in the r and z directions, respectively.

These equations were considered in the axisymmetrical configuration, with calculations performed between the spacers ends and limited to half of the system cross-section (see Fig. 1).

Initial and boundary conditions

An effective electric current I_{RMS} is imposed on the upper surface of the system and the electric potential is zero at its lower surface. To better reproduce the desired thermal sintering cycle, a PID module reproducing the closed-loop controller configuration has been programmed and integrated into the finite element software. The current intensity is calculated considering the difference, e(t), between prescribed and calculated temperatures at control point A (see Fig. 1), as follows:

$$I_{RMS}(t) = K_P \times e(t) + K_I \times \int_0^t e(\tau)d\tau + K_D \times \frac{de(t)}{dt} \quad (3)$$

where K_P, K_I and K_D are respectively the proportional, integral and derivative gains, adjusted for an optimum control response.

The initial temperature of the simulations was fixed at 27 °C and two main heat transfer boundary conditions were applied:

(i) Due to heat removal by water cooling, a conducto-convective flux, q_c, across the upper and lower horizontal surfaces was considered and expressed by:

$$q_c = h_c(T_s - T_w) \quad (4)$$

where h_c is the conducto-convective coefficient, T_w the water temperature (27 °C) and T_s the horizontal surface temperature.

(ii) As the experiments were conducted in vacuum, the lateral surfaces of the device suffer losses only by radiation according to the following equation:

$$q_r = \sigma_s \varepsilon \left(T_e^4 - T_a^4\right) \quad (5)$$

where q_r is the radiation heat flux, σ_s is the Stefan-Boltzmann constant, ε is the emissivity of the lateral surfaces, T_e is the emission surface temperature (graphite) and T_a is the chamber wall temperature.

The sample was considered as fully dense and the alumina properties used in the model are those given in the Ref. [5].

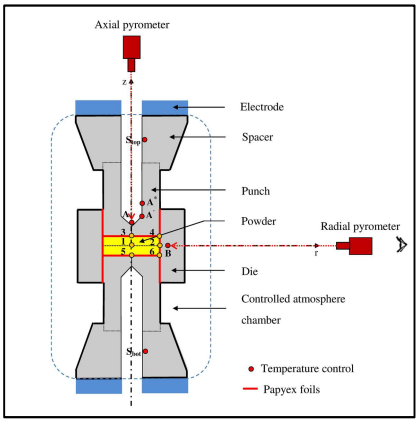

Fig. 1: Sketch in a 2D view of SPS set-up with locations of the temperature measurements devices (points A, A', A*, B, S_{top} and S_{bot}) and reference locations in the sample.

3-Results and discussion

3.1-SPS experiments results

Multiple samples were processed for 20 and 40 mm diameters at the same SPS processing conditions. In these experiments, a dissymmetry in water cooling at the bounds of the SPS device is noticed. From the obtained results of experiments for the thinner samples (2.5 mm in final thickness), as shown in Table 1, it can be noticed that a dispersion of temperature measurements exists at the control point B (position B in Fig. 1). This dispersion, in terms of the measurements results, may be related to: the deviation of the light beam alignment of the control optical pyrometer (position A in Fig. 1) and the die asymmetric location relatively to the sample. Both incidents or at least one may occur during the experimental runs influencing the experimental conditions retained for materials sintering. Modeling with these incidents, in the case of a symmetrical water cooling at the bounds of the device, does permit to explain the discrepancies observed for measuring at position B (at 3 mm the sample side) for both configurations ϕ20 and ϕ40.

Table 1: Experimental values of temperature T_A and T_B at control positions A and B respectively, during dwell time and under the same processing conditions.

Sample	T_A (°C)	T_B (°C)	T_A–T_B (°C)
ϕ20	1300	1282	18
		1273	27
		1268	32
ϕ40	1300	1283	17
		1272	28

3.2-Effect of the temperature control location

Concerning the first to the non-repeatability of temperature measurements during SPS experiments, we studied the influence of the positioning of the control optical pyrometer at different axial location A* (A* is not fixed, varying relatively to the upper surface of the sample) on the maximum temperature reached in the SPS system as shown in Fig. 2.

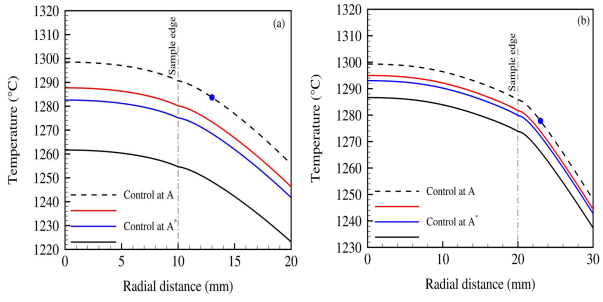

Fig. 2: Radial temperature distributions for ϕ20 (a) and ϕ40 (b) diameters in function of the temperature control

location at point A (reference location) and at point A*. Solid symbols correspond to the measured temperature at position B on the die.

Fig. 2a (ϕ20) and 2b (ϕ40) show the control location effect on the radial temperature distributions along sample-die assembly and on the maximum temperature reached at the sample center during the SPS sintering cycle. In fact, at point A, positioned at 4 mm above the powder/punch interface, the maximum temperature reached in sample center is order of 1298.5 °C and 1299.3 °C for ϕ20 and ϕ40 diameters respectively, near the onset temperature (1300 °C), in contrast when the control pyrometer is located at point A* (6 mm from point A' in Fig. 1), the temperature values are order of 1261.7 °C and 1286.6 °C for ϕ20 and ϕ40 diameters respectively. It is noted that, the farther away the control location is from the reference point A, the more the temperature distribution decreases along the radial direction and also the temperature at the measuring point T_B decreases. By contrast, along the central radial line 1-2, the thermal gradient in the sample ($\Delta T_{12} = T_1 - T_2$) remains the same (order of 8 °C and 13.5 °C for 20 and 40 mm diameters respectively).

3.3-Effect of the die asymmetric location

The die asymmetric location, relatively to the sample, is a situation quite common that happens during SPS experiments, related to lining up sample-punches-die assembly before the sintering in the SPS setup. A case study was done where the die is shifted slightly upward or downward causing asymmetric punches-die assembly. Seven cases were considered for the diameters ϕ20 (Fig. 3a) and ϕ40 (Fig. 3b) in the case of thinner samples (2.5 mm in final thickness): die centered location (dashed line in Fig. 3), die shifted by ranging of 1 to 3 mm upward, denoted d^+(mm) (thin lines in Fig. 3) and downward, denoted d^-(mm) (thick lines in Fig. 3).

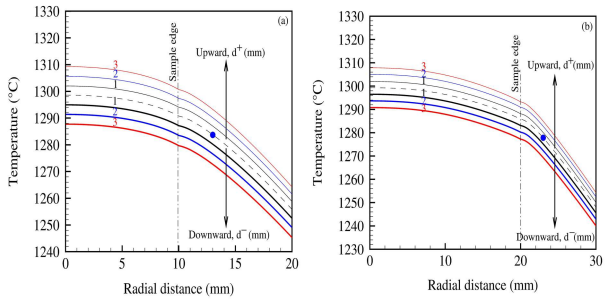

Fig. 3: Radial temperature distributions for ϕ20 (a) and ϕ40 (b) diameters in function of the die location. Solid symbols correspond to the measured temperature at position B on the die.

The radial temperature distributions along sample and die presented in Fig. 3 demonstrate that for diameter ϕ20 (Fig. 3a), the maximum temperature reached at the sample center is about 1309.3 °C to 1287.7 °C, for a die shift by 3 mm upward and downward respectively. On the contrary, in the case of the diameter ϕ40 (Fig. 3b), the maximum temperature reached at the sample center is about 1307.8 °C to 1290.8 °C for the utmost shifts. The temperature inside the sample increased when the die is shifted upward from the centered location. However, the radial temperature gradient is not affected by this change in die location. Accordingly, optical pyrometer, placed at borehole spot area (3 mm of diameter) drilled on the die, is slightly above or below the median plan of the sample after sintering.

4-Conclusion

In this paper, investigations were undertaken to elucidate the experimental conditions affecting the reproducibility of temperature measurements during Spark Plasma Sintering process. The overall conclusions of the conducted work can be summarized as follows:

-Numerical FEM models permit to reproduce the thermoelectric phenomena occurring during the SPS process, and have proven to be interesting sources of information on inaccessible experimental data.

-Serious difficulties arise when trying to position the sensors and devices (thermocouples and optical pyrometers) to monitor or to control the temperature during the SPS process.

-Temperature control and die asymmetric location relatively to the sample affect strongly the experimental conditions for materials densification by SPS sintering.

References

[1] R. Orrù, R. Licheri, A.M. Locci, A. Cincotti, G. Cao, *Consolidation/Synthesis of Materials by Electric Current Activated/Assisted Sintering*, Mater. Sci. Eng. R 63 (2009) 127-287.

[2] O. Guillon, J.G. Julian, B. Dargatz, T. Kessel, G. Schierning, J. Räthel, M. Herrmann, *Field-Assisted Sintering Technology/Spark Plasma Sintering: Mechanisms, Materials, and Technology Developments*, J. Adv. Eng. Mater. 16 (2014) 1-20.

[3] T. Voisin, L. Durand, N. Karnatak, S. Le Gallet, M. Thomas, Y. Le Berre, J.F. Castagne, A. Couret, *Temperature Control during Spark Plasma Sintering and Application to Up-Scaling and Complex Shaping*, J. Mater. Process. Technol. 213 (2013) 269-278.

[4] C. Wolff, *Modélisation du Processus Electro-Thermo-Mécanique de Frittage Flash*, Ph.D. Dissertation, Paul Verlaine University, 2011, Metz.

[5] S. Muñoz, U. Anselmi-Tamburini, *Temperature and Stress Fields Evolution during Spark Plasma Sintering Processes*, J. Mater. Sci. 45 (2010) 6528-6539.